RSC Advances

REVIEW

View Article Online
View Journal | View Issue

Cite this: *RSC Adv.*, 2022, **12**, 23057

Gold nanocrystals: optical properties, fine-tuning of the shape, and biomedical applications

Meng Li, *[a] Jianlu Wei,[b] Yang Song [a] and Feiyong Chen*[a]

Noble metal nanomaterials with special physical and chemical properties have attracted considerable attention in the past decades. In particular, Au nanocrystals (NCs), which possess high chemical inertness and unique surface plasmon resonance (SPR), have attracted extensive research interest. In this study, we review the properties and preparation of Au NCs with different morphologies as well as their important applications in biological detection. The preparation of Au NCs with different shapes by many methods such as seed-mediated growth method, seedless synthesis, polyol process, ultrasonic method, and hydrothermal treatment has already been introduced. In the seed-mediated growth method, the influence factors in determining the final shape of Au NCs are discussed. Au NCs, which show significant size-dependent color differences are proposed for preparing biological probes to detect biomacromolecules such as DNA and protein, while probe conjugate molecules serves as unique coupling agents with a target. Particularly, Au nanorods (NRs) have some unique advantages in the application of biological probes and photothermal cancer therapy compared to Au nanoparticles (NPs).

Received 9th July 2022
Accepted 29th July 2022

DOI: 10.1039/d2ra04242h

rsc.li/rsc-advances

1. Introduction

Nobel metal nanoparticles (NPs) are widely applied in numerous fields. Among various noble metal nanomaterials, Au nanomaterials, which possess high chemical inertness and unique surface plasmon resonance (SPR) have gained extensive interest and research.[1–3] Au nanocrystals (NCs) are studied comparatively early and have attracted increasing attention in medical and biological research because of their special physical and chemical properties and bio-affinity.[4] It has been proven that Au NCs can be prepared *via* a simple preparation procedure with good control over particle size, stable chemical properties, good biocompatibility, as well as easy to modify with biomolecules. Therefore, Au NCs have been proposed for applications in genomics,[5] biosensors,[6–8] clinical chemistry,[9] cancer cell photothermal therapy,[10–14] optical imaging techniques,[15,16] targeted delivery of drugs, antigens, peptides, DNA, and so on.[17–19]

The interesting optical properties of Au NCs result from the excitation of free electron plasmons by the electromagnetic field.[1,20–22] The plasmon modes of Au NCs are determined by

[a]*Resources and Environment Innovation Institute, Shandong Jianzhu University, Jinan, 250101, P. R. China. E-mail: mengli_ujn@163.com; ctokyo@hotmail.com*

[b]*Department of Orthopaedic Surgery, Qilu Hospital Shandong University, 107 Wenhua Xi Road, Jinan, 250012, P. R. China*

Meng Li achieved her doctoral degree at School of Materials Science and Engineering in University of Jinan. She got a PhD training at Chemistry Department in the University of Texas at San Antonio as an visiting scholar from 2018 to 2019. Her research mainly based on the preparation and applications of nanomaterials and published 18 relative articles. She is currently working at the School of Institute of Resources and Environmental Innovation in Shandong Jianzhu University.

Jianlu Wei achieved his PhD and Doctor degree from Shandong University. Additionally, he got PhD training in New York University as an exchange scholar from 2013 to 2016. Dr Jianlu Wei finished his postdoc training in Hebei Medical University. So far, Dr Jianlu Wei expertized in spinal surgery and published 16 relative articles. Corresponding address is the Department of Orthopaedics, Shandong University Qilu Hospital, Jinan, Shandong, 250012, China.

shape, composition, size, and surrounding media. The resonance frequency is very sensitive to the shape of the NCs. In particular, Au nanorods (NRs) are promising systems for optical studies, as the spectrum is easily tunable by varying the aspect ratio.[2,23,24] As such, it is crucial to have tight control over the size and crystal structure of Au NCs.[25–27] As a face-centered cubic (fcc) metal, Au NCs with different shapes have been synthesized successively.[28–33] In realistic chemical synthesis, many critical parameters including thermodynamic and kinetic parameters are responsible for the final shapes of Au NCs. Shape control synthesis provides one of the most powerful means to tailor the properties of Au NCs.[34,35]

Due to extensive research and the importance of Au NCs, various reviews related to the preparation and applications of Au NCs have been published over the years.[36–43] Most of them provided a specific introduction to various aspects of Au NCs, such as photosynthesis, modification, functionalization, toxicity of Au NCs, as well as the application of Au NCs in therapeutic applications, targeted drug delivery, and energy or environment.[36–40,43,44] A few publications are providing a generalized introduction to the synthesis, properties, and applications of Au NCs.[4,44,45] In particular, there is still a lack of detailed understanding of the synthesis mechanism or the precise controlling of the reaction parameters, which may prevent us from realizing the full potential of synthetic approaches and accurately controlling the growth of Au NCs. The specific physicochemical and optoelectrical characteristics of Au NCs are closely related to their size and morphology, which can be controlled by the selection of a synthetic approach.[38,46,47] The understanding of the reaction process and mechanism is promising to choose the appropriate synthesis route and reaction parameters such as time, temperature, and pH according to the required characteristics. Due to the frequently reported publications on Au NCs, this review may be incomplete and should be regarded as the starting point for understanding the basic principles behind the synthesis, properties, and biomedical applications of Au NCs.

In this review, the properties and preparation of Au NCs with different morphologies as well as their important applications in biological detection are summarized. The preparation of Au NCs with different shapes by many methods such as seed-mediated growth method, seedless synthesis, the polyol process, ultrasonic method, and hydrothermal treatment is introduced. For the widely reported seed-mediated growth method, the influencing factors in determining the final shape of Au NCs were studied. Some of the advantages and disadvantages of chemical synthesis methods are discussed, as well as the green synthesis methods are highlighted. The main objective of the present work is to provide a better basis for the synthesis, properties, and biomedical applications of Au NCs, which is beneficial for the further development of Au NCs.

2. Properties of Au NCs

Seo *et al.* reported that surface energy has a strong influence on the physical and chemical properties of the materials and there was a significant negative correlation between the ratio of surface atoms *versus* total volume and surface energy.[25] It must be mentioned that bulk Au has distinct yellowish color, and the size dependence of the color of colloidal Au is simply the consequence of how light interacts with matter.[20–22] NCs, typically in the size range of 1–100 nm, possess size and shape-dependent properties, which differ from their bulk behavior. The color of the colloidal dispersions of Au NCs in a fluid, typically water, varies from red to blue, depending upon the shape and size of the particles. For example, spherical colloidal Au NCs with a diameter of around 10 nm produce aqueous dispersions with a ruby red color, while increasing their size to nearly 100 nm or changing the morphology to rod-like (length 30 nm, diameter 10 nm) results in making the colloidal

Yang Song received his PhD in Urban Environmental Systems from Chiba National University in 2015. He is currently a Professor at the Institute of Resources and Environmental Innovation of Shandong Jianzhu University. His work focuses on the use of catalytic methods to solve energy and environment problems, and has organized or presided over 19 major scientific research projects. He was awarded the National Outstanding Self-funded Scholarship for International Students in 2016, and won the first prize of the technical group of the National Postdoctoral Academic Forum on Biological Industry Development and Culture and People's Livelihood.

Feiyong Chen received his PhD in Civil Engineering from Tokyo Institute of Technology in 1996. He was elected as a Foreign Associate of The Engineering Academy of Japanese in 2018 and was elected as a Pearl River Scholar of Guangdong Province in 2019. He is currently the Dean and Professor of the Institute of Resource and Environmental Innovation, Shandong Jianzhu University. He has long been engaging in scientific research and engineering practice in the fields of environment pollution control and prevention, environment ecological planning and restoration, and has organized or presided over more than 100 major engineering in more than 20 countries.

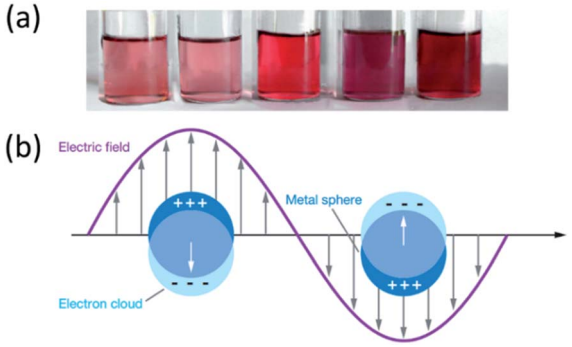

Fig. 1 (a) Photograph of the colloids 3, 4, 6, 9, and 35 nm (from left to right) of Au NPs. Reproduced from ref. 49 with permission from Elsevier, copyright [2008]; (b) schematic illustrating a localized surface plasmon. Reproduced from ref. 50 with permission from Annual Reviews, copyright [2007].

dispersion appear bluish.[48] Fig. 1(a) shows the photograph of Au NPs with sizes 3, 4, 6, 9, and 35 nm (from left to right).[49]

The research interest in Au NCs over the past decades has been stemming from their remarkable optical properties related to SPR. SPR comes from the excitation of free electron plasmon by the electromagnetic field.[1–3] When light impinges on Au NCs, free electrons of Au NCs interact with the incident light and produce resonance coupling. The oscillation leads to the charge separation between free electrons and the metal core, producing a coulomb force, such that the electrons oscillate around the surface of the particles.[50] Fig. 1(b) illustrates the localized surface plasmon.[50] SPR is produced when the vibration frequency of the incident light and free electrons are equal. SPR causes a strong absorption peak in UV-vis absorption spectroscopy. Optical absorption peaks of Au NCs appeared in the wavelength range of 510–550 nm, and the resonance frequency is very sensitive to the shape of NPs.

3. Synthesis of Au NPs

Au NCs, as a face-centered cubic (fcc) metal, are known to have enclosed by low-index {100}, {111}, and {110} facets. The relative surface energies are in the order of $\gamma\{111\} < \gamma\{100\} < \gamma\{110\}$.[25] This phenomenon results from the rapid elimination of the high-index facets with the addition of atoms during the Au NC formation process.[26] The rate of crystal growth in the direction perpendicular to a high-index facet is generally much faster than that along the normal direction of a low-index facet, which results in the rapid elimination of the high-index facets with the addition of atoms during the formation of NCs.[26,51] As a result, in solution chemistry, fcc metal NCs enclosed by low-index {100}, {111} and {110} facets are more commonly observed because of their relatively low surface energy.[52]

The physical and chemical properties were controlled by the shape of Au NCs.[25,27] Xia *et al.* mentioned that Au NCs, which possess high-index facets on their surface, such as trisoctahedral and concave cubic, showed better electro-catalytic activity in comparison to that possessing only low-index facets.[53] This phenomenon can be explained by the reason that the high-index facets of a single crystal possess a high density of low-coordinated atoms such as steps, edges, and kinks, which can be served as highly active sites for adsorption and even catalysis.[27,54,55]

As a symmetric fcc structure, it is not easy for Au to form single-crystal multi-armed NCs in isotropic aqueous solutions. Nevertheless, Chen *et al.* provided a systematic introduction to the preparation methods of monopod, bipod, tripod, and tetrapod Au NCs.[71] To date, Au NCs with different shapes as spheres,[28–30] rods,[31–33,73] cubes,[29,74] triangle,[53] polyhedron[25,59] and others[34,75] have been synthesized successively. Such as those in the TEM or SEM images of Au NCs with different morphologies shown in Fig. 2.

There are many methods to prepare Au NCs, such as conventional chemical synthesis, polymer-mediated synthesis, UV-induced photochemical synthesis, ultrasound-assisted synthesis, laser ablation synthesis, and microbial-mediated synthesis.[76–82] The solution-based chemical route produces a number of structural architectures, from the quasi-spherical, triangle, concave cubic, hexagon, truncated tetrahedra, octahedra, rhombic dodecahedra, trisoctahedra, decahedra, icosahedra, rod-like to tetrapod, star-like, and branched structures in high yield. Fig. 3 shows the general synthetic conditions of different methods for the preparation of Au NCs with typical morphologies.

The most typical method for preparing colloidal gold is the sodium citrate reduction method. Colloidal gold of different sizes can be prepared by changing the type and concentration of the reducing agent.[83] In general, parameters are responsible for the final shapes of noble metal NCs. The synthetic method, reagents used in the growth process, the temperature of synthesis, reaction time, dimensions, and yield of Au NCs with different shapes are illustrated in Table 1.

In solution-based chemical synthesis, thermodynamic and kinetic parameters controlled the growth of NCs.[26,84] Thermodynamic parameters include temperature and reduction potential, while kinetic parameters include reactant concentration, diffusion, solubility, and the reaction rate. By controlling these parameters, it is possible to tune the nucleation and growth stages of NCs and achieve crystallographic control.

The seed-mediated growth method is the widely reported method in conventional chemical synthesis.[85,86] Since its inception and application, the seed-mediated growth method has made a revolutionary impact on the majority of the reported synthesis of shape-controlled Au NCs. It is typical that the seed-mediated growth process comprises the preparation of small Au NCs and subsequent growth in reaction solutions.[87,88] Both, the crystallinity of seeds and the growth rates of different crystallographic facets play a vital role in determining the final shape of the resultant nanostructure.[89]

The shape of Au NCs could be controlled by tuning nucleation and growth stages in the seed-mediated growth method.[26,90,91] In the solution-phase synthesis of NCs, "nucleation" can be broadly defined as the formation of a small cluster from atoms in the solution. Small Au seed particles are generated under conditions of high chemical supersaturation. This leads to the fastest nucleation rate. Once the nuclei have grown

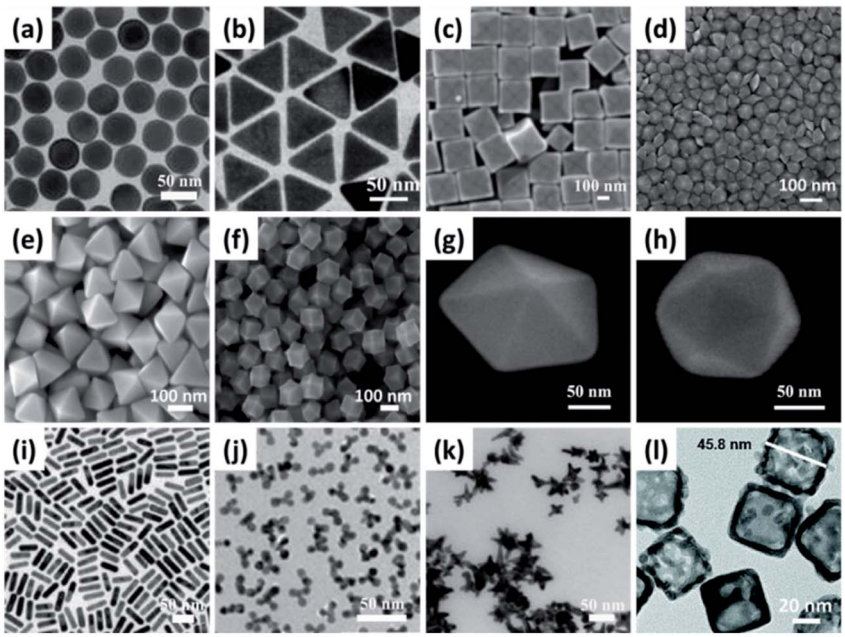

Fig. 2 (a, b, i, j, k and l) TEM images of Au nanostructures with different shapes: (a) spherical (b) triangle (i) rod-like (j) tetrapod (k) starlike (l) nanocage. (c–h) SEM images of Au nanostructures with different shapes: (c) concave cubic (d) hexagonal bipyramid (e) octahedral (f) rhombic dodecahedra (g) decadron (h) icosahedral. (a) Reproduced from ref. 29 with permission from American Chemical Society, copyright [2010]; (b) reproduced from ref. 56 with permission from American Chemical Society, copyright [2014]; (c) reproduced from ref. 57 with permission from American Chemical Society, copyright [2010] (d) reproduced from ref. 58 with permission from American Chemical Society, copyright [2013] (e and f) reproduced from ref. 59 with permission from American Chemical Society, copyright [2008] (g and h) reproduced from ref. 25 with permission from American Chemical Society, copyright [2008] (i) reproduced from ref. 31 with permission from American Chemical Society, copyright [2012] (j) reproduced from ref. 60 with permission from American Chemical Society, copyright [2014] (k) reproduced from ref. 61 with permission from American Chemical Society, copyright [2014] (l) reproduced from ref. 62 with permission from the Royal Society of Chemistry, copyright [2017].

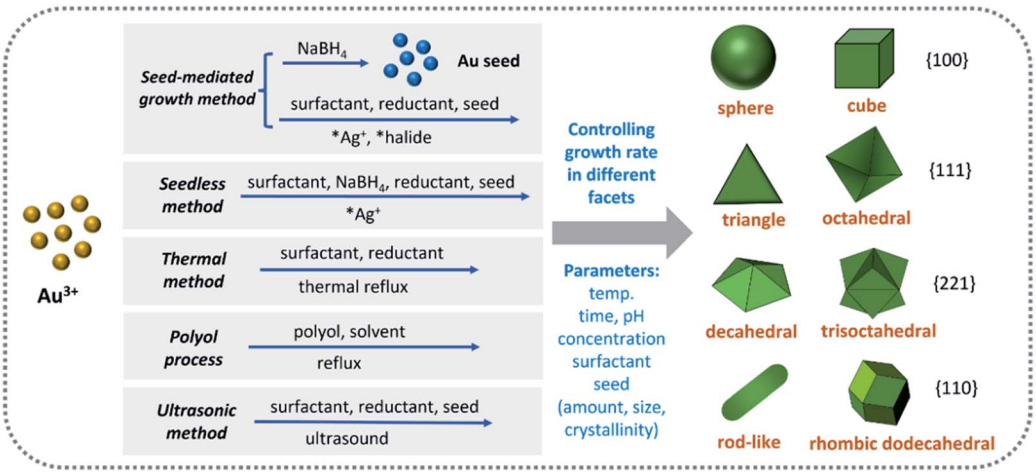

Fig. 3 The general synthetic conditions of different approaches for the preparation of Au NCs with different morphologies. (*Optional).

past a critical size, they will have relatively stable crystallinity and well-defined crystallographic facets exposed on their surface, which can be termed "seeds". The shape of a seed is primarily determined by the minimization of the surface energy.[85]

After the nucleation stage, each type of seed can still grow into an NC with several possible shapes. The reaction conditions are then altered and more Au ions and the reductant are added, together with some form of a shape-templating surfactant or molecule, and the seeds are grown into larger particles of particular morphologies or habits. The final shape is controlled by the growth rates of different facets.[89] As the seed grows into a nanocrystal, the growth rates of different facets can be altered with capping agents to control the final shape.

Table 1 Synthesis of Au NCs with different morphologies[a]

Morphology	Synthetic method	Reagents	Temp. (°C)	Reaction time	Dimension (nm)	Yield (%)	Ref.
Sphere	Seedless method	$HAuCl_4$, AA, $NaBH_4$, CTAC	28	Overnight	~7–27	100	53
Triangle	Seed-mediated, growth method	CTAB, $HAuCl_4$, AA	RT	N/A	35	80	63
Concave cubic	Seedless method	$NaBH_4$, $HAuCl_4$, AA, CTAC, HCl, $AgNO_3$	28	Overnight	~62.3–173	95	53
Cube	Seed-mediated, growth method	CTAB, $HAuCl_4$, AA, ($AgNO_3$)	RT	N/A	85 (70)	85	63
	Seed-mediated, growth method	KBr, $HAuCl_4$, CPC-capped seed, CPC	30	120 h	55.7	96.1	59
	Seedless method	CTAB, $HAuCl_4$, AA, $NaBH_4$	28	Overnight	~10–65	N/A	53
	Thermal method	$AuCl_3$, DDAB, $NaBH_4$, dodecylthiol, octyl ether	100	a few minutes	~10	N/A	64
Hexagon	Seed-mediated, growth method	CTAB, $HAuCl_4$, AA	RT	N/A	70	90	63
Tetrahedral	Polyol process	PVP, $HAuCl_4$, DEG	200	25 min	~210–290	60	25
Octahedral	Seed-mediated, growth method	$HAuCl_4$, AA, CPC-capped seed, CPC	30	120 min	53.4	97.2	59
	Hydrothermal method	CTAB, $HAuCl_4$	160	600 min	50	90	65
Rhombic dodecahedral	Seed-mediated, growth method	$HAuCl_4$, AA, CPC-capped seed, CPC	30	120 min	53.4	100	59
	Seed-mediated, growth method	$HAuCl_4$, $NaBH_4$, CTAB, AA, 4-ATP	30	120 min	120	72	27
Trisoctahedral	Seedless method	CTAC, $HAuCl_4$, AA, $NaBH_4$	28	180 min	~50–250	95	53
	Seed-mediated, growth method	CTAC, $HAuCl_4$, AAs	28	N/A	~55–120	90	63 and 66
Decahedral	Polyol process	PVP, $HAuCl_4$, DEG	245	10 min	~48–90	80	25
	Ultrasonic method	$HAuCl_4$, PVP, Au seed	RT	N/A	~35–65	80–90	67 and 68
Icosahedral	Polyol process	PVP, $HAuCl_4$, DEG	245	10 min	94	N/A	25
Rod-like	Seed-mediated, growth method	CTAB, $HAuCl_4$, AA	25	180 min	Width: 6~42, length: 22~475	97	63, 69 and 70
	Seedless method	CTAB, $HAuCl_4$, AA, $NaBH_4$, $AgNO_3$	28	180 min	Width: ~11, length: ~46	98	53
Tetrapod	Seed-mediated, growth method	CTAB, $HAuCl_4$, AA, ($AgNO_3$)	RT	N/A	293(30)	75(70)	63
Star-like	Seed-mediated, growth method	CTAB, $HAuCl_4$, AA	30	720 min	66	95	63, 71 and 72

[a] RT: room temp.; N/A: unmentioned. 4-ATP: 4-aminothiophenol; DDAB: didodecyldimethylammonian bromide; PVP: poly(vinylpyrrolidone); CTAB: cetyltrimethylammonium bromide; CTAC: cetyltrimethylammonium chloride; DEG: diethylene glycol; AA: ascorbic acid.

Typically, the growth stage is much slower and proceeds under milder reducing conditions than those at the nucleation stage.[92] The shaping of these nanostructures can be analyzed by the deposition of metal atoms on the seed surface under reductive environments.[25] Grzelczak *et al.* proclaimed that in comparison to the nucleation stage, the growth stage was under a milder reducing process and the reaction rate was much slower.[92,93]

Some chemical stabilizers such as poly(vinyl pyrrolidone) (PVP), poly(vinyl alcohol), and sodium dodecyl sulfate are added to reaction mixtures to control the growth of Au NCs.[94–96] Polyhedral Au NCs with decahedral, icosahedral, and truncated tetrahedral shapes are synthesized by a simple one-pot polyol process in the presence of PVP.[97,98] A high PVP concentration of up to 360 equivalent of the Au precursor, $HAuCl_4$, effectively stabilizes decahedral seeds to yield uniform decahedra with various edge sizes. Decreased PVP concentration subsequently leads to selective formation of icosahedral and truncated tetrahedral.[25,99] At relatively low PVP concentration, the internal surface energy of the crystals becomes more important than the interaction energy between surface atoms and PVP, and the particles prefer more rounded shapes to reduce the total surface area. The icosahedral structure is close to spherical and has stable {111} facets on the surface. The edge truncation of the icosahedron helps to diminish its structural strain energy.[25]

Typical reducing agents such as citric acid, borohydride, tetrafluoroborate, AA are used during the preparation of Au NCs.[94,100,101] AA is a commonly used reducing agent during the preparation of Au NCs. However, it has been reported that Au NCs can be obtained in large quantities by the aspartate reduction of Au ions. Suri *et al.* put forward amines as an attractive class of reducing agents because of their universal presence in biology and the environment.[102] Dong *et al.* described that amino acids can control the size and morphology of the Au NCs. They mentioned that amino acid moieties could form an organic matrix to have an influence on the biomolecules and inorganic materials.[103]

Conventional synthesis techniques involving the seed-mediated growth method, seedless method, polyol process, hydrothermal method, and ultrasonic method have been developed for the synthesis of Au NCs with different sizes and shapes. Chemical methods can generate Au NCs at a low cost and provide repeatable results using various chemicals. Although the chemical synthesis methods described above are effective, many of them suffer from some drawbacks such as high temperature, harsh reaction conditions, long reaction times, the use of toxic and aggressive chemicals as reducing and/or capping agents to control the size and composition of Au NCs, resulting in the environmental pollution caused by the use of organic solvents.[104–107] Besides, the toxic capping agents or chemicals used in the synthesis process tend to adsorb on the surface of Au NCs, which may cause severe threats to living cells while using Au NCs for drug delivery and diagnostic applications.[108–112] Consideration of the environmental problems, Firdhouse *et al.* summarized the detailed advantages and disadvantages of conventional synthesis techniques for Au NPs synthesis.[113]

In view of the environmental impact, eco-friendly green synthesis methods have currently become popular.[114–120] Current strategies of ''green'' concern include the use of nontoxic chemicals, biodegradable polymers, and environmentally benign solvents.[121] In the green synthesis methods, the extracts from living organisms such as leaves, stems, roots, seeds, flowers, fruit, whole plant, fungi, and algae are available as reducing and capping agents.[121,122] The synthesis of Au NCs *via* green routes has the advantages of simplicity, economical friendliness, low cost, moderate reaction conditions, and application of non-toxic chemicals.[114,123,124] This technique provides a wide range of applications for functional nanomaterials because ascorbic acid, terpenes, alkaloids, phenols, polyphenols, and flavonoids are coated on the surface of NCs, resulting in Au NCs with lower toxicity than chemically synthesized counterparts. Not only that, Au NCs showed enhanced solubility and stability due to coating with biomolecules.[125] Nevertheless, the green synthesis methods are possibly related to some major operational obstacles, such as the need for a longer time, critical downstream processing to purify nanoparticles in high yields, and difficulty to optimize the process parameters and expand the scale.[126,127]

4. Synthesis of Au NRs

One-dimensional Au nanostructures have received considerable attention due to their size-dependent optical, catalytic, and electronic properties.[128,129] The research interest in Au NRs over the past decades has stemmed from their anisotropic configuration and unique optical properties. Since its inception and commercialization, Au NRs have made a revolutionary impact in the field of bioanalysis and have become a powerful tool for bioanalytical chemistry.

Shape control provides one of the most powerful tools to tailor the properties of noble metal nanostructures. In Fig. 4(a), *L*/*D* is the aspect ratio. Fig. 4(b) is the photograph of the

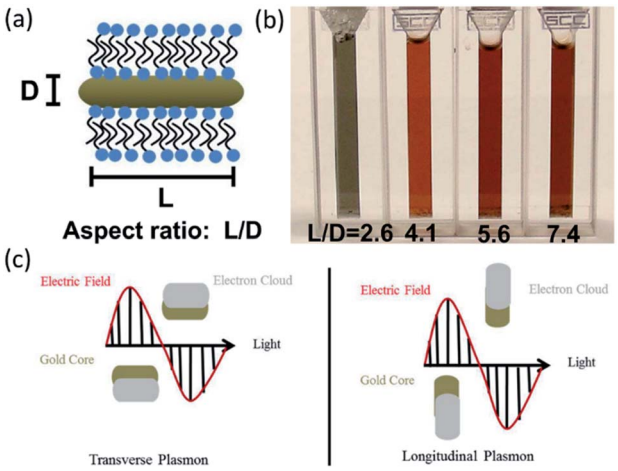

Fig. 4 (a) Au NRs possess two separate plasmon absorbances, one corresponding to the short ("transverse") axis and the one corresponding to the longitudinal axis. *L*/*D* is the aspect ratio. Reproduced from ref. 24 with permission from American Chemical Society, copyright [2013]; (b) photograph of colloidal Au prepared in water. Aspect ratios are 2.6, 4.1, 5.6, and 7.4 (from the left), respectively. Reproduced from ref. 20 with permission from Elsevier, copyright [2009]; (c) schematic representation of transverse and longitudinal plasmon absorbances in Au NRs. Reproduced from ref. 24 with permission from American Chemical Society, copyright [2013].

colloidal solution of Au NRs. The color of the colloidal solution is related to the aspect ratios of Au NRs. There are distinct differences between the spherical Au NPs and Au NRs. The distinct difference from spherical NPs is that Au NRs possess two distinct surface plasmon resonances; a transverse SPR corresponding to the short axis of the rod, and a longitudinal SPR corresponding to the long axis (Fig. 4(c)). The energy of the longitudinal SPR can be tuned from the middle of the visible region of the electromagnetic spectrum (~600 nm) to the infrared region (~1800 nm), simply by changing the aspect ratio of the Au NRs.[23,24]

Au NRs have been prepared by conventional wet chemistry, photochemical and electrochemical methods.[130] Among the reported procedures, the seed-mediated growth has been by far the most efficient and popular approach. Au NRs are prepared by a seed-mediated growth approach, which uses ~4 nm Au nanoclusters as seeds and subsequent reduction of a metal salt with a weak reducing agent in the presence of a directing surfactant to produce NRs.[128] Besides the seed-mediated growth method, seedless synthesis is the other typical synthetic method to prepare Au NRs. The difference between the seed-mediated growth method and seedless synthesis is that the sizes of *in situ* seeds grown using $NaBH_4$ are about 1.5 nm, while the sizes of the seeds used in the seed-mediated growth method are about 3.5 nm. The seedless method with a size of about 1.5 nm is in favor of the synthesis of anisotropic Au NCs.[1,131] The dimension of Au NRs prepared by the seedless synthesis method is about 25 × 6 nm, while about 60 × 15 nm by the seed-mediated growth method.[132] The size of Au NRs produced by seedless synthesis is much smaller than that prepared by the seed-mediated growth method.[133–135]

The seed-mediated growth method is discussed in detail in the following part.

The seed-mediated growth method is a typical growth process that involves the preparation of Au NRs. Many factors affect the growth of Au NRs, such as the concentration of reagents, the pH of the growth solution, and the type of the directing surfactant. Table 2 lists the influencing factors on the growth of Au NRs. In the solution-phase synthesis, impurities or capping agents can change the order of free energies of different facets through their interaction with a metal surface. As a result, the facet with a slower growth rate will be exposed more on the surface.[89]

4.1 There are many factors affecting the growth of Au NRs

4.1.1 Directing surfactant. A surfactant such as CTAB plays a crucial role in the growth process of Au NRs. It seems that the growth of an NR takes place simultaneously in all directions. Once the seed grows to a critical size, the facets become large enough for significant surfactant binding. The growth rate of different facets in the presence of the surfactant determines the final shape of the nanoparticle. The slower growth in the width of the NR is an example of better protection of {110} facets by CTAB. The growth and the final size of Au NRs depend on the Au supply and the surfactant concentration. In general, the surfactant is much higher in concentration; this process continues until the Au supply depletes.[23]

The original idea was to use micelles formed by the cationic surfactant CTAB as a "soft template" to direct NR formation.[20] Previous studies suggested that CTAB formed a bilayer on the surface of NR.[136,137] Compared to the ends, the assembly of CTAB bilayers along the long faces of Au NRs is preferred. Besides, CTAB assists in the fine-tuning of the shape because CTAB preferentially binds to the middle of the NRs. This property makes it possible to form Au NRs with a dog-bone shape.[128]

It has been demonstrated that decreasing the concentration of CTAB yielded the NRs with shorter aspect ratios (1 to 6).[142] On the contrary, employing a surfactant with a longer aliphatic surfactant and smaller seed solution obtained longer NRs.[142] In 2005, citrate-capped Au NPs were chosen as seeds for Au NRs growth.[1] Then, Liu and Guyot-Sionnest observed differences between the crystalline structures of citrate and CTAB-stabilized seeds, confirming the multiply-twinned structure of citrate-capped seeds.[1]

A careful choice of the experimental conditions allows the growth of the seeds into NRs. Factors including temperature,[20] pH,[144,146,149,150] crystallinity of seed particles,[1,151] concentration of reactants,[128,150,151] single-component surfactants other than CTAB,[152] binary surfactant mixtures,[23] aromatic additives,[31] and the presence of iodide ions in the growth solution[142,147,148] have been carefully evaluated by several research groups.

4.1.2 Seed. The amount added and the size of the seed impact the aspect ratio of Au NRs. The aspect ratio of Au NRs could be precisely controlled through the careful variation of the added amount of the seed into the growth solution. For a constant concentration of reagents, increasing the size of the seed decreased the aspect ratio of Au NRs.[131]

4.1.3 Reducing agent. AA as a mild reducing agent has been widely used in the seed-mediated growth method. Vivek Sharma *et al.*[20] introduced that the reduction process of the Au ion by AA that can be described as:

First reduction:

$$Au^{3+} \rightarrow Au^{+}$$

$$CTA\text{–}AuBr_4 + C_6H_8O_6 \rightarrow CTA\text{–}AuBr_{2+}C_6H_6O_6 + 2H^{+} + 2Br^{-}$$

Second reduction:

Table 2 The impact of factors on Au NRs in the seed-mediated growth method[a]

Parameter	Influence factors	Mechanism	Effect on products	Reference
Directing surfactant	CTAB: concentration	Growth rate in different facets	Morphology, AR, morphology	20 and 136–138
	A binary surfactant mixture	Growth rate in different facets	Uniformity, yield, AR, width	23
Au ions	Concentration	Growth rate	Length	23
Ag ions	Concentration	Interact with surfactant	Length, AR, yield	23 and 139–141
Seed	Amount	Growth rate	Size, AR	131
	Crystallinity (Citrate-capped: multiply-twinned) (CTAB-capped: single crystal)	Binding with surfactant	Morphology, dimension, crystallinity, yield, AR	1 and 92
	Size	Growth rate	Size, shape, AR	131 and 142
Reducing agent (AA)	The molar ratio of AA to Au	Reaction rate	AR, yield	20
	Temperature	Reduction rate	Morphology, AR	20
	pH	Reduction rate, reducing power	Morphology, yield, AR	20, 87 and 142–146
Halide ions	Molar ratio	Growth rate in different facets	Morphology	142, 147 and 148
Aromatic additives	Cationic CTAB micelles	CTAB-aromatic additive systems	AR, yield, monodispersity	31

[a] AR: aspect ratio.

$$Au^{+} \rightarrow Au^{0}$$

$$CTA\text{–}AuBr_2 + C_6H_8O_6 \rightarrow 2Au + C_6H_6O_6 + 2CTA^{+} + 2H^{+} + 4Br^{-}$$

The overall reaction is:

$$2CTA\text{–}AuBr_4 + 3C_6H_8O_6 \rightarrow 2Au + 3C_6H_6O_6 + 2CTA^{+} + 6H^{+} + 8Br^{-}$$

The first reduction is confined to the metal micelles. The second reduction starts only after the addition of the seed solution. The study on the effect of the concentration of AA on the growth of Au NRs indicated that the reaction rate becomes faster with the increasing in the concentration of the reducing agent. The decrease in the reaction rate was in favor of the isotropic growth, thereby increasing the yield of NRs. The reduction rate affects the morphology of NRs. For example, an insufficient amount of AA yielded fatter Au NRs.[20]

4.1.4 Temperature and pH. Apart from the reducing agent, both the temperature and pH are also able to change the morphology of Au NRs by controlling the reduction rate. The former report demonstrated that the aspect ratio of Au NRs increased with the decrease in the temperature.[20] It is worth noting that the increase in the aspect ratio is due to a decrease in the diameter of NRs. The decrease in the diameter resulted from the effective confinement of the growth in the short axis at low temperature.[20]

The pH value affects the reduction rate and reduces the power of the reducing agent. AA has a much weaker reducing power in a strongly acidic solution than in a weakly acidic solution.[87,143] Adding a small amount of the HCl solution to the growth solution could decrease the whole reduction rate and increase the aspect ratio.[153,154] The feasible formation of Au nanoprisms with an addition of a small amount of NaOH has been observed in a previous report by Mirkin *et al.*[155] This is because the reducing power of AA can be enhanced by eliminating the proton produced by the reduction.[145] Therefore, the formation of nanoprisms can be promoted at higher pH values. In other words, the chemical potential of AA is maintained at a higher state after the addition of NaOH.[142]

4.1.5 Au and Ag ions. Increasing the aspect ratio of Au NR with the increase in the Au atom content of the growth solution indicates that the higher the concentration of the Au former the longer the NRs. However, a further increase in the concentration of the Au ions caused the decrease in the length of the NRs because of the formation of Au–Br-surfactant.[23]

The effect of the silver ion content does not always increase the aspect ratio of Au NRs. The negative effects of higher concentrations of silver ions may be due to their interaction with the bromide-resistant ions of the surfactant monomer.[23] Babak *et al.* explored the role of silver in the growth process of Au NRs and reported that Ag^{+} could first increase and then decrease the length of Au NRs, similar to the effect of Au ions.[23]

Liu and Guyot-Sionnest proposed an elaborate explanation for the role of Ag^{+}.[1] They suggested that the under-potential deposition (UPD) of metallic silver occurs on different crystal facets of Au NCs, leading to symmetry breaking and rod formation. UPD is an important process that occurs during the formation of metallic layers on metallic substrates.[156] It is widely observed that when a metal working electrode is slowly cathodically polarized, a second noble metal ion can be deposited on the substrate to form a thin film.[157] Crucially, the initial deposition of metal monolayers with potentials much higher than the Nernst potential of the deposited metal is often observed. This deposition of the first and sometimes the second monolayer is called UPD. Ag^{+} UPD does occur on Au {111} and the UPD process is influenced by the presence of chloride ions.[92] In the presence of Cl^{-}, the UPD offset becomes stronger.

The above mechanism does not work in the growth of Au NRs using surfactant templates because the added silver ions are not reduced to atomic silver. Both silver ions and Au ions were contained in the growth solution, and AA as a reducing agent can only reduce the Au ions. Only under a basic pH, AA has the ability to reduce silver ions.[140] The deposition of silver on the surface of Au NRs only happens at pH $\geq$ 8 in the CTAB solution, with AA as the reducing agent.[158] Jana *et al.* reported that the preparation of Au NRs in the absence of silver ions can only obtain Au NPs.[139] This result confirmed that Ag^{+} adsorbed on the surface of Au NPs in the form of AgBr restricts the growth and stabilizes the NR surface.

The question that remains unresolved is why the addition of $AgNO_3$ during the growth of Au NRs leads to an increase in the yield and greatly improves the control of the aspect ratio of Au NRs. If the silver ion has catalytic activity and promotes the formation of NRs, the length should not be improved and only the number of NRs would increase. In fact, Ag^{+} could combine with the headgroups of the capping material such as CTAB to form Ag–Br pairs. Ag^{+} as a complexing agent between the monomers assists the template elongation.[141] Ag–Br pairs, which are formed between $AgNO_3$ and CTAB adsorbed in the facets of Au NPs cause restriction, limiting their growth, and obtaining Au NRs.[23] This combination decreases the charge density on the bromine ion, resulting in less repulsion between adjacent head groups on the gold surface. The repulsion between the neighboring headgroups results in CTAB template elongation.

4.1.6 Halide ions. Halide ions influence the growth of Au NPs during the seed-mediated growth using CTAB as a cationic surfactant. The presence of distinct halide ions and their molar ratios resulted in the formation of diverse morphologies, such as spheroid, nanoplates, or NRs.[159] The dramatic change of the morphology is related to the adsorption of halide on different surfaces.[160] Chung *et al.* showed that a small amount of iodide ion resulted in the triangular nanoprisms in the presence of excessive bromide ion, in its absence, NRs were the main products.[142] The main effect of iodide ions is to decrease the overall rate of crystal growth, and iodide adsorption appears to inhibit crystal growth along the Au (111) direction, resulting in triangular nanoprisms.[142] In addition, a minuscule amount of iodide ion is crucial for the formation of a triangular disk

instead of NRs. All halide ions are specifically adsorbed on low-index Au surfaces such as (111), (110), and (100).[142] Robert *et al.* demonstrated that Cl ions are important for shape controlling of Ag NPs.[161]

4.1.7 Binary surfactant mixture. Using a binary surfactant mixture consisting of CTAB and benzyldimethylhexadecylammonium chloride (BDAC) in a seed-mediated method resulted in Au NRs with good uniformity, higher yield, and fewer by-products.[23,162,163] However, this effect was not observed in pure BDAC or large ratios of BDAC/CTAB mixture.[164] The growth solution only containing BDAC caused the formation of the nanosphere. This indicates that the CTAB monomer is necessary for the growth of NRs, and these monomers are more affected by silver ions.[23] This could be attributed to the smaller size and polarizability of chloride ions than bromine ions. Therefore, compared with Ag–Br, the bond in Ag–Cl is expected to be weak. As the contribution of BDAC increases, the average width of NR decreases.

5. Biomedical applications

Metal and semiconductor NCs show different characteristics, which are usually different from their corresponding bulk materials. NCs with a high surface area can enter cells and interact with intracellular substances. In recent years, metal and semiconductor NCs with new or improved optical, electrical and magnetic properties have attracted wide interest in basic research and biomedical applications.[165–168] Semiconductor NPs consist of a few atoms up to several thousand atoms. The electronic energy level will be quantized when its size is small enough (typically less than 10 nm), in this case, they are also named quantum dots (QDs).[169] Yang *et al.* mentioned that QDs possess high photoluminescence efficiency and have unique applications in biological and light-emitting devices.[170] QDs have attracted significant interest due to their small size and high fluorescence quantum yield.[171] However, possible applications in biomedical fields are limited by their toxicity.

Compared to toxic QDs, Au NCs have good biological applications in single cell research due to their good stability, cell permeability, and easy coupling with biological macromolecules. Besides, the diameter of Au NCs is in the range of 1–100 nm, and most biological molecules (such as proteins and nucleic acids) are in this size range.[167] Milkin *et al.* mentioned that nanomaterials are attractive probe candidates because of the following four reasons. First, they have a small size (1–100 nm) and a large specific surface area. Second, physical and chemical properties can be adjusted by controlling the size, composition, and shape of NCs. Then, they unusually target binding properties. Finally, they have overall structural robustness.[176] Based on the above properties, Au NCs can be used as probes to detect the physiological functions of biological molecules and reveal the life process at the molecular level. The typically biomedical applications of Au NCs in sensing, imaging, therapy, and immunology are presented in Fig. 5.

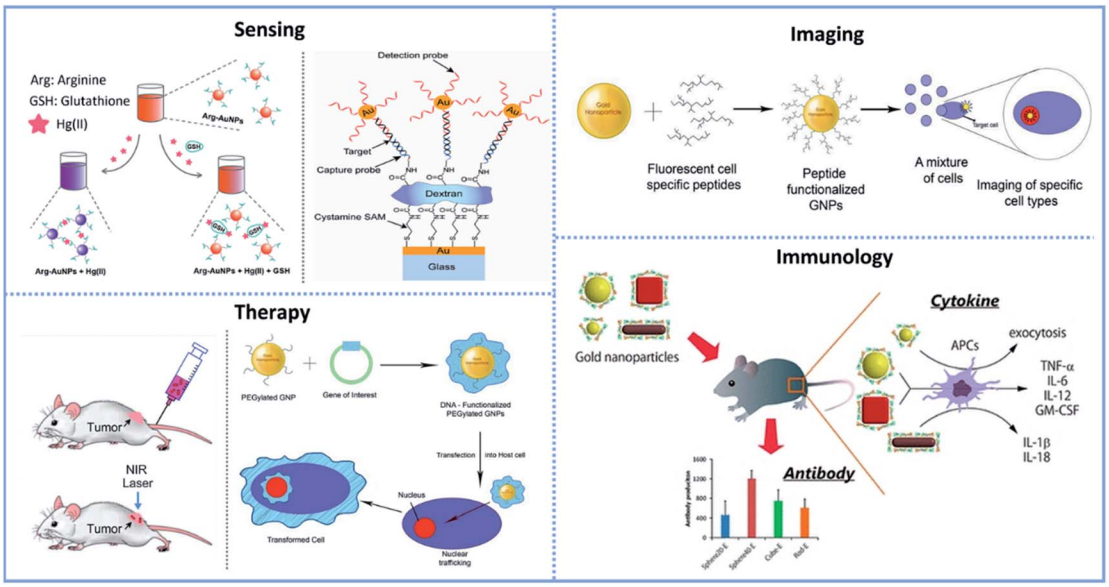

Fig. 5 Summary of the typically biomedical applications of Au NCs. *Sensing application*: (left) arginine-modified Au NPs for GSH sensing in cell cancer are distributed and regulated by a chromogenic approach. Reproduced from ref. 172 with permission from John Wiley and Sons, copyright [2015]; (right) schematic representation of the sandwich DNA detection assay *via* Au NP-mediated SPR signal amplification. Reproduced from ref. 173 with permission from Elsevier, copyright [2006]. *Imaging application*: Au NPs functionalized with cell-specific peptides for bioimaging. Reproduced from ref. 174 with permission from MDPI (Basel, Switzerland), copyright [2011]. *Therapy application*: (left) scheme of the photothermal destruction of an implanted tumor in a mouse after injection of Au NRs functionalized with poly(ethylene glycol). Reproduced from ref. 16 with permission from Royal Society of Chemistry, copyright [2011]; (right) functionalized Au NPs for gene delivery. Reproduced from ref. 174 with permission from MDPI (Basel, Switzerland), copyright [2011]. *Immunology application*: the antigen-based West Nile Virus Protein (WNVE) is attached to PSS-MA coated Au NPs (different sizes and forms) through electrostatic activity directed to virus vaccinations. Reproduced from ref. 175 with permission from American Chemical Society, copyright [2013].

5.1 Biomedical applications of Au NPs

The electronic energy levels of Au NPs are split owing to their small size. The distance between the energy levels is related to the size of NPs. Specific wavelength light absorption occurs when the electron transition from a low band gap to a high band gap, resulting in the solution presenting different colors.[177] The color of colloidal Au is related to the size of Au NPs.[178,179] The color changes from pale orange-yellow, wine red, deep red, blue, and purple with the increase in the particle size. Its unique color change is the basis of biochemical applications.[177,180]

The properties of colloidal Au mainly depend on the diameter and surface characteristics of Au NPs. They have controllable surface chemical properties for modification with various chemical and biologically active molecules.[181] It has been reported that the affinity of Au NPs with various sizes and shapes to thiols, disulfides, dithiocarbamates, and amines allows bioconjugation with many kinds of biological molecules.[182] The above characteristics provide the possibility for the detection of specific DNA and proteins.[183] Due to the good biocompatibility of Au, colloidal Au can be used for biological labels and the determination of protein concentration.

The SPR of Au NPs is extremely sensitive to the environment, size and shape.[181,182] The aggregation degree, particle size range, and morphology of Au NPs can be determined by UV-visible absorption spectroscopy. The characteristic absorption peaks of Au NPs appeared at 510–550 nm. Under normal conditions, the surface of Au NPs is negatively charged, and the electrostatic repulsion between particles is greater than the van der Waals force. Therefore, a certain distance between the particles is maintained and the solution remains stable. When the external conditions change, such as lowering the temperature or adding the electrolyte solution, it would lead to aggregation between particles, resulting in the SPR absorption peak red shift.[180] For example, the color of colloidal Au changes, and the absorption spectrum red-shifts while Au NPs are absorbed by biomacromolecules and the distances between the particles are smaller than their diameters.[16,48] These are the principles for the detection of DNA and proteins.[16]

With the discovery of immune Au labelling, Au NPs began to be used in biomedical applications in the 1970s.[184] All the nano gold probes mentioned here were based on citrate-stabilized anionic Au NPs. Since the 1980s, Au NPs, which are connected with biomacro-molecules, have been used for various analytical methods.[16] In 1980, the sol particle immunoassay was proposed by Leuvering *et al.*[185] In 1996, Mirkin *et al.* proposed to use the assembled Au NPs with thiol-modified oligonucleotides as biological probes to detect DNA.[186–188] Subsequently, a large number of reports using colorimetric assay methods to detect DNA, antigen and biological molecules, using Au nanoprobes decorated with oligonucleotides, antibodies, peptides have appeared.

The colorimetric assay method has become an attractive choice for biological detection because it does not require the use of advanced equipment and is easy to operate in many applications. When particles aggregate to a certain extent, the color of the solution changes dramatically. Plasmon resonance absorption peak red-shifts when the target molecule hybridizes with functional groups to cause the colorimetric response, indicating the presence of the target molecule.[16,186] Colorimetric methods have high selectivity and sensitivity for particle size, shape, and structure.[15,176]

In the colorimetric assay method, the surface of Au NPs was functionalized. Glomm W. R. and Khlebtsov *et al.* referred to "functionalization" as defined as biomacromolecules attached to the surface of Au NPs.[189,190] Physical adsorption and coordination bond coupling are the two main methods to combine Au NPs with biological macromolecules, such as single-stranded oligonucleotides, antibodies, peptides, and carbohydrates.[16,184,186,191] Au NPs are used as optical markers, as well as probe-conjugated molecules for coupling with the target. Functionalization is the basis of biological applications.[16] In general, Au NPs were decorated with intermediate linkers so that they could be functionalized. The most commonly used intermediate linkers are thiol or thiolated derivatives, which are connected by the Au–S bond. In addition to alkylthiols, other ligands such as phosphine, amino, and carboxyl groups can also be used as linkers.[192,193]

Genetic testing contains two contents including gene sequence identification and point mutation determination. Gene sequence identification may be used for genetic diagnosis. Point mutation determination is of great importance in the diagnosis of genetic diseases and drug resistance.[194] There are two strategies for detecting DNA using the colorimetric method: one is based on the conjugation of 10–30 nm Au NPs with thiol-modified single-stranded oligonucleotides (ssDNA), and the other uses the unmodified Au NPs as Au nanoprobes.[186,195–198] The main process of preparing Au NPs for DNA detection is as follows: first, a thiol-modified oligonucleotide is synthesized. Then, oligonucleotides are added to the Au solution to form a solid connection with the surface of Au NPs through an Au–S covalent bond. Finally, buffer solution with an appropriate concentration should be added. After centrifugation, the nano-gold probe is obtained.[182,195] The complex process is time-consuming. It is unstable in the presence of a buffer solution because of the aggregating effect of salt ions, but Au NPs are readily stabilized by functionalization.[182] Rothberg *et al.* designed a gene detection method without the surface modification of Au NPs.[196,199] Colloidal Au remains stable due to electrostatic repulsion between particles. When a small amount of electrolyte solution, such as NaCl solution, is added, the electrostatic repulsion between nanoparticles is shielded by the electrolyte solution, resulting in particle aggregation and color change. There are some different propensities between ssDNA and double-stranded oligonucleotides (dsDNA). Due to van der Waals force, ssDNA can be adsorbed on the surface of Au NPs and remain stable at relatively high electrolyte concentrations. However, dsDNA presents a negatively charged phosphate skeleton, so dsDNA does not adsorb on the surface of negatively charged Au NPs.[200] Therefore, after adding ssDNA or dsDNA and a certain concentration of salt solution to nano-gold solution, the color of adding ssDNA remained red, while the color changed from red to blue in the presence of dsDNA.[196,201]

In addition, nano gold probes can be used to detect the mismatch of base pairs.[180,202] Taton *et al.* created a solid-phase detection mode based on the gold nanoprobe to identify target genes.[203] In colorimetric analysis, the solution color changed from red to blue when the growth solution contained the target gene. After the formation of the three-dimensional network structure, the system temperature gradually increased. When the temperature increases to a certain extent, the mismatched base pairs degenerated. As a result, the distance between particles returned to the distance before aggregation, and the color of the solution gradually returned to red. On the contrary, the completely complementary ssDNA remained stable, and the solution color did not change at this temperature. Therefore, this method can be used to detect point mutation.

Nanogold probes can be used for the detection of proteins.[204,205] Au NPs were easily decorated using thiolate chemistry and their optical properties depend on the size.[206] Citrate-protected Au NPs, which are conjugated with proteins such as antibodies are used in biomolecular detection.[207] However, in a salt environment, citrate-protected Au NPs tend to aggregate. It is surprising that they are not easy to aggregate after being connected with the protein layer. This method can be used to confirm the successful connection between Au NPs and proteins.[208] Au NPs have strong adsorption with proteins and other biological macromolecules. As a consequence, there is a good prospect in the immune analysis.

5.2 Biomedical applications of Au NRs

In addition to Au NPs, Au NRs also have been used in biological fields due to their strong light scattering efficiency, stable optical characteristics and are easy to process, and they are a good molecular probe because of the polarized light. Because of their anisotropic configuration and unique optical properties, Au NRs have great potential in chemical and biochemical sensing such as for metal ions, amino acids, antibodies, cancer cell imaging, and photothermal therapy.[130,166,195,209–214] In addition, Au NRs have the advantages of strong optical signals, high photostability and can be easily synthesized and engineered so that they can be used as single-molecule optical probes. More importantly, Au NRs whose light absorption and scattering are polarized are suitable for probe orientations.

A typical Au nano-solution is hydrophobic and thermodynamically unstable, which requires surfactant stability.[190] Au NPs synthesized by reducing $HAuCl_4$ usually have negative charges on their surface. In contrast, Au NRs synthesized by the seed-mediated growth method are stabilized by CTAB, which is a widely used cationic surfactant and has a positive charge on its surface. In contrast to Au NPs, it is difficult for Au NRs to be functionalized due to the presence of CTAB surfactant molecules serving as stabilizers. Nevertheless, Dujardin *et al.* obtained a specific organization of short Au-NRs into anisotropic three-dimensional (3D) aggregates by DNA hybridization, but in this approach, it is needed to remove excess surfactant after the synthesis of Au NRs.[215] Although CTAB bilayers hinder the formation of the Au–S bond between thiol-modified DNA and Au NRs, there exists electrostatic interaction between the positively charged ammonium of CTAB and the phosphate backbone of the DNA.[216] Since the Au NR surface has a positive charge, it can connect with the negatively charged un-modified ssDNA and dsDNA through electrostatic interactions.[217] This is the most fundamental difference between Au NPs and Au NRs.[218]

There are mainly three methods to displace CTAB from the surfaces of Au NRs or harness the electrostatic interactions between CTAB and DNA.[216] One approach is to control the electrostatic interactions between DNA and positively charged surfaces.[16,195,219] The second approach is through packing the NRs with a thin film of silica. The outer silica layers were modified with DNA functionalized by amine or thiol. The third approach is using the ligand exchange process to decorate Au NRs with ss-DNA.[216,220]

CTAB-coated Au NRs were able to withstand high salt concentrations even without decorations and deposits.[221,222] He *et al.* described the use of un-modified CTAB-coated Au NRs for colorimetric assay. In this approach, it is not necessary to remove the excess CTAB from the solution by centrifugation.[195] It only needs the addition of target DNA to the mixture of the Au NRs without any modification and the label-free probe DNA in certain buffer salt solutions. The SPR absorption band will red-shift in a high ionic strength buffer after mixing the NR probe and target ssDNA, indicating the aggregation of Au NRs. This phenomenon is ascribed to the formation of dsDNA from hybridization between the target DNA and probe DNA. In contrast, the addition of noncomplementary targets will not cause any spectral changes.[16,195] This protocol only experiences one step and is very simple for detecting hybridization. Moreover, it is easy to detect single-base-pair mismatches without temperature control, providing promising applications in the detection of single-nucleotide polymorphisms (SNPs) and disease diagnosis.[195,223,224] Although Au NRs have unique advantages in biological application, few studies applied Au NRs as orientation probes. The reason may come from the following reasons. First, there is a lack of good preparation and processing methods to obtain the desired size. Broader functionalities and applications can be achieved by tuning the longitudinal plasmon band of Au NRs.[225] Second, there is no suitable imaging technique to decipher its three dimensions.

Au NRs have shown potential in photothermal cancer therapy and optoelectronic technology.[134,226,227] In 2004, O'Neill *et al.* demonstrated that Au NRs with SPR absorption in the near-infrared (NIR) region can target tumors *in vivo*. After excitation with a NIR laser, Au NRs released heat into the tumor environment, resulting in the rupture of the tumor cell membrane.[228] After that, Huang *et al.* reported that Au NRs with a low aspect ratio can be used as a simultaneous imaging and therapeutic agent to promote tumor cell recognition and photothermal removal *in vitro* due to their strong scattering and absorption properties in NIR spectroscopy.[229] The demonstration greatly increases the interest in the treatment and diagnosis of certain cancers using Au NRs. Compared with traditional chemotherapy, photothermal therapy may become an effective and specific cancer treatment option. Ideally, cell

death can only be induced in the region where Au NRs are excited by laser with appropriate wavelengths.[229–231] Photothermal therapy has attracted tremendous attention in killing cancer cells, making it a promising biomedical candidate for the treatment of cancer. In recent years, using assembled Au NRs for the photothermal killing of bacteria has also shown promising prospects.[232]

6. Conclusions and outlook

6.1 Conclusions

In this study, we focused on the properties and preparation of Au NCs with different morphologies as well as their important applications in biological detection. The ability to carefully tailor the physical properties of Au NCs such as sizes, shapes, and composition is essential for their biomedical applications. As a face-centered cubic (fcc) metal, Au NCs can take a variety of geometrical shapes. In realistic chemical synthesis, particularly in the solution phase, many critical parameters, which can be divided into thermodynamic and kinetic parameters are responsible for the final morphologies of Au NCs. The seed-mediated growth method is the widely reported method, both the crystallinity of seeds and the growth rates of different crystallographic facets play a vital role in determining the final shape of a resultant nanostructure.

The colorimetric assay method has become an attractive choice for biological detection because it does not require the use of advanced equipment and is easy to operate in many applications. Nanogold probes including citrate-coated Au NPs and CTAB-coated Au NRs are being used for biological detection, such as oligonucleotides, proteins, and enzymes. Citrate-protected Au NPs can be easily decorated *via* thiolate chemistry and their optical properties depend on their size. In addition to Au NPs, Au NRs also have been used in biological fields. Since the Au NR surface has a positive charge, it can connect with the negatively charged un-modified ssDNA and dsDNA through electrostatic interactions. There are some disadvantages while using Au NCs in the colorimetric assay method. For example, it requires complex experimental procedures and cannot monitor the hybridization process real-time. In addition, it could not be achieved for absolute quantitative analysis. Therefore, it is important to find a simple, real-time, and quantification system.

6.2 Perspective and challenge

The chemical method can generate Au NCs at a low cost and provide repeatable results using various chemicals. Gold NPs are considered an important research field due to their unique and tunable SPR and their application in biomedical science, including drug delivery, tissue/tumor imaging, photothermal therapy, and immunochromatography identification of pathogens in clinical specimens. The synthesis of Au NCs with such extended medical applications should be free from toxic chemicals used during the synthesis process. It is promising to develop a green, effective, simple, air-stable, and cost-effective technique for the synthesis of Au NCs. The tendency of the presented approach is: (i) without the usage of a surfactant, capping agent, or template; (ii) the selection of an environmentally acceptable solvent with the use of eco-friendly reducing and stabilizing agents, for example, replacing toxic chemicals with extracts from living organisms for the synthesis of Au NCs; (iii) excellent yield of the products; (iv) simple maintenance and reuse of the Au NCs. For Au NCs synthesized using chemical methods, functionalizing the surface with more peculiar ligands to regulate and detoxify, which is caused by the toxic capping agents, is encouraged. These are the few future aspects for the generation of NCs *via* green synthesis and many more are yet to be explored by researchers.

As for the application, gold nanoprobes are facing many challenges, such as selectivity and sensitivity decrease, reduction of the catalytic activity, and potential biohazard, in the practical application. To address these challenges, the existing detection technology should be further improved, and new functional nanoprobes should be developed on the basis of practical problems. In addition, more sensitive and easier methods of analysis should be designed. Along with further research, it is our ultimate goal to achieve automatic and intelligent sample testing. While using Au NRs as probes, developing a suitable imaging technique to decipher its three dimensions is expected. We hope that our research efforts in this review will contribute to a better understanding of the synthesis, optical properties, shape tuning, and applications of Au NCs.

Author contributions

Meng Li conceived the study and collected the literature. All authors were involved in writing and revising the manuscript.

Conflicts of interest

There are no conflicts to declare.

Acknowledgements

This work was supported by the projects from Shandong Top Talent Special Foundation; National Key Research and Development Program of China (No. 2022YFE0105800); The Introduction and Cultivation Plan for Young Innovative Talents of Colleges and Universities by the Education Department of Shandong Province; Nanxun Collaborative Innovation Center Key Research Project (No. JZ2022ZH01); Doctoral research fund project in Shandong Jianzhu University (X22033Z); the Open-ended Fund of Key Laboratory of Urban Pollutant Conversion, Chinese Academy of Sciences (KLUPC KF-2020-4).

References

1 M. Liu and P. Guyot-Sionnest, *J. Phys. Chem. B*, 2005, **109**, 22192–22200.
2 D. Yin, X. Li, Y. Ma and Z. Liu, *Chem. Commun.*, 2017, **53**, 6716–6719.

3 E. Yeo, U. J. Cheah, D. Neo, W. I. Goh, P. Kanchanawong, K. C. Soo, P. S. Thong and J. Kah, *J. Mater. Chem. B*, 2017, **5**, 254–268.
4 S. Menon, R S. and VK S., *Resource-Efficient Technologies*, 2017, **3**, 516–527.
5 X. Liu, Q. Dai, L. Austin, J. Coutts, G. Knowles, J. Zou, H. Chen and Q. Huo, *J. Am. Chem. Soc.*, 2008, **130**, 2780–2782.
6 S. Gupta, S. Huda, P. K. Kilpatrick and O. D. Velev, *Anal. Chem.*, 2007, **79**, 3810–3820.
7 Q. L. Wang, H. F. Cui, C. L. Li, X. Song, Q. Y. Lv and Z. Y. Li, *Sensors and Actuators Reports*, 2020, **2**, 100021.
8 Z. Yang, A. S. Malinick, T. Yang, W. Cheng and Q. Cheng, *Sensors and Actuators Reports*, 2020, **2**, 100023.
9 P. Baptista, E. Pereira, P. Eaton, G. Doria, A. Miranda, I. Gomes, P. Quaresma and R. Franco, *Anal. Bioanal. Chem.*, 2008, **391**, 943–950.
10 X. Huang, P. K. Jain, I. H. El-Sayed and M. A. El-Sayed, *Lasers in Medical Science*, 2008, **23**, 217–228.
11 S. Lal, S. E. Clare and N. J. Halas, *Acc. Chem. Res.*, 2008, **41**, 1842–1851.
12 W. Il Choi, J. Kim, C. Kang, C. C. Byeon, Y. H. Kim and G. Tae, *ACS Nano*, 2011, **5**, 1995–2003.
13 S. Siddique and J. C. L. Chow, Gold Nanoparticles for Drug Delivery and Cancer Therapy, *Appl. Sci.*, 2020, **10**, 3824.
14 R. A. Barmin, P. G. Rudakovskaya, O. I. Gusliakova, O. A. Sindeeva, E. S. Prikhozhdenko, E. A. Maksimova, E. N. Obukhova, V. S. Chernyshev, B. N. Khlebtsov and A. A. Solovev, *Nanomaterials*, 2021, **11**, 415.
15 N. G. Khlebtsov and L. A. Dykman, *J. Quant. Spectrosc. Radiat. Transfer*, 2010, **111**, 1–35.
16 L. Dykman and N. Khlebtsov, *Chem. Soc. Rev.*, 2012, **41**, 2256–2282.
17 F. Farzaneh, M. R. Rashidi and O. Yadollah, *Talanta*, 2018, **192**, 118–127.
18 T. Xue, W. Liang, Y. Li, Y. Sun, Y. Xiang, Y. Zhang, Z. Dai, Y. Duo, L. Wu, K. Qi, B. N. Shivananju, L. Zhang, X. Cui, H. Zhang and Q. Bao, *Nat. Commun.*, 2019, **10**, 28.
19 A. Graczyk, R. Pawlowska, D. Jedrzejczyk and A. Chworos, *Molecules*, 2020, **25**, 204.
20 V. Sharma, K. Park and M. Srinivasarao, *Mater. Sci. Eng., R*, 2009, **65**, 1–38.
21 Z. Yang, Z. Li, X. Lu, F. He, X. Zhu, Y. Ma, R. He, F. Gao, W. Ni and Y. Yi, *Nano-Micro Lett.*, 2017, **9**, 5.
22 M. Yang, Y. Liu, W. Hou, X. Zhi, C. Zhang, X. Jiang, F. Pan, Y. Yang, J. Ni and D. Cui, *Nanoscale*, 2017, **9**, 334–340.
23 B. Nikoobakht and M. A. El-Sayed, *Chem. Mater.*, 2003, **15**, 1957–1962.
24 S. E. Lohse and C. J. Murphy, *Chem. Mater.*, 2013, **25**, 1250–1261.
25 D. Seo, C. I. Yoo, I. S. Chung, S. M. Park, S. Ryu and H. Song, *J. Phys. Chem. C*, 2008, **112**, 2469–2475.
26 W. Niu and G. Xu, *Nano Today*, 2011, **6**, 265–285.
27 H. E. Lee, K. D. Yang, S. M. Yoon, H. Y. Ahn and K. T. Nam, *ACS Nano*, 2015, **9**, 8384–8393.
28 A. Henglein and D. Meisel, *Langmuir*, 1998, **14**, 7392–7396.
29 Y. Zheng, X. Zhong, Z. Li and Y. Xia, *Part. Part. Syst. Charact.*, 2013, **31**, 266–273.
30 P. Suchomel, L. Kvitek, R. Prucek, A. Panacek and R. Zboril, *Sci. Rep.*, 2018, **8**, 4589.
31 X. Ye, L. Jin, H. Caglayan, J. Chen, G. Xing, C. Zheng, V. Doan-Nguyen, Y. Kang, N. Engheta and C. R. Kagan, *ACS Nano*, 2012, **6**, 2804–2817.
32 M. Censabella, M. G. Grimaldi and F. Ruffino, *Mater. Charact.*, 2019, **147**, 101–115.
33 M. Brown and B. J. Wiley, *Chem. Mater.*, 2020, **32**, 6410–6415.
34 A. McLean, M. Kanetidis, T. Gogineni, R. Ukani, R. McLean, A. Cooke, I. Avinor, B. Liu, P. Argyrakis, W. Qian and R. Kopelman, *Chem. Mater.*, 2021, **33**, 2913–2928.
35 L. Z. Wang, *J. Phys. Chem. B*, 2012, **104**, 1153–1175.
36 M. Yaseen, M. Humayun, A. Khan, M. Usman, H. Ullah, A. A. Tahir and H. Ullah, *Energies*, 2021, **14**, 1–88.
37 A. Sani, C. Cao and D. Cui, *Biochem. Biophys. Rep.*, 2021, **26**, 100991.
38 N. Sarfraz and I. Khan, *Chem.–Asian J.*, 2021, **16**, 720–742.
39 X. Y. Liu, J. Q. Wang, C. R. Ashby Jr, L. Zeng, Y. F. Fan and Z. S. Chen, *Drug Discovery Today*, 2021, **26**, 1284–1292.
40 M. H. Mohd-Zahid, R. Mohamud, C. A. C. Abdullah, J. Lim, H. Alem, W. N. W. Hanaffi and I. Z. Alias, *RSC Adv.*, 2020, **10**, 973–985.
41 K. Nejati, M. Dadashpour, T. Gharibi, H. Mellatyar and A. Akbarzadeh, *J. Cluster Sci.*, 2022, **33**, 1–16.
42 L. Tessaro, A. Aquino, A. P. A. de Carvalho and C. A. Conte-Junior, *Sensors and Actuators Reports*, 2021, **3**, 100060.
43 T. Ahmad, J. Iqbal, M. A. Bustam, M. Irfan and H. M. Anwaar Asghar, *J. Cleaner Prod.*, 2021, **309**, 127460.
44 R. Herizchi, E. Abbasi, M. Milani and A. Akbarzadeh, *Artif. Cells, Nanomed., Biotechnol.*, 2016, **44**, 596–602.
45 N. Elahi, M. Kamali and M. H. Baghersad, *Talanta*, 2018, **184**, 537–556.
46 I. Kherbouche, Y. Luo, N. Félidj and C. Mangeney, *Chem. Mater.*, 2020, **32**, 5442–5454.
47 M. T. Yaraki and Y. N. Tan, *Chem.–Asian J.*, 2020, **15**, 3180–3208.
48 C. J. Murphy, A. M. Gole, S. E. Hunyadi, J. W. Stone, P. N. Sisco, A. Alkilany, B. E. Kinard and P. Hankins, *Chem. Commun.*, 2008, **18**, 544–557.
49 D. Philip, *Spectrochim. Acta, Part A*, 2008, **71**, 80–85.
50 K. A. Willets and R. P. Van Duyne, *Annu. Rev. Phys. Chem.*, 2007, **58**, 267–297.
51 S. Xu, X. Dong, S. Chen, Y. Zhao, G. Shan, Y. Sun, Y. Chen and Y. Liu, *Sens. Actuators, B*, 2019, **281**, 375–382.
52 R. Rajendra, P. K. Gangadharan, S. Tripathi, S. Kurungot and N. Ballav, *Nanoscale*, 2016, **8**, 19224–19228.
53 J. Zhang, C. Xi, C. Feng, H. Xia, D. Wang and X. Tao, *Langmuir*, 2014, **30**, 2480–2489.
54 G. Mettela, R. Boya, D. Singh, G. Kumar and G. U. Kulkarni, *Sci. Rep.*, 2013, **3**, 1793.
55 L. Karuppasamy, C. Y. Chen, S. Anandan and J. J. Wu, *Electrochim. Acta*, 2017, **246**, 75–88.
56 L. Chen, F. Ji, Y. Xu, L. He, Y. Mi, F. Bao, B. Sun, X. Zhang and Q. Zhang, *Nano Lett.*, 2014, **14**, 7201–7206.

57 J. Zhang, M. R. Langille, M. L. Personick, K. Zhang, S. Li and C. A. Mirkin, *J. Am. Chem. Soc.*, 2010, **132**, 14012–14014.
58 M. L. Personick, M. R. Langille, J. Wu and C. A. Mirkin, *J. Am. Chem. Soc.*, 2013, **135**, 3800–3803.
59 W. Niu, S. Zheng, D. Wang, X. Liu, H. Li, S. Han, J. Chen, Z. Tang and G. Xu, *J. Am. Chem. Soc.*, 2009, **131**, 697–703.
60 C. Kai, S. R. Kothapalli, H. Liu, L. K. Ai, J. V. Jokerst, J. Han, Y. Meng, J. Li, J. Levi and J. C. Wu, *J. Am. Chem. Soc.*, 2014, **136**, 3560–3571.
61 D. Dam, R. C. Lee and T. W. Odom, *Nano Lett.*, 2014, **14**, 2843–2848.
62 C. Yan, L. Cui, Q. Yang, X. Zhou, L. Pan, X. Zhang, H. Yang, Z. Zhou and S. Yang, *J. Mater. Chem. B*, 2017, **5**, 8761–8769.
63 T. K. Sau and C. J. Murphy, *J. Am. Chem. Soc.*, 2004, **126**, 8648–8649.
64 R. Jin, S. Egusa and N. F. Scherer, Thermally-Induced Formation of Atomic Au Clusters and Conversion into Nanocubes, *J. Am. Chem. Soc.*, 2004, **126**(32), 9900–9901.
65 Y. Huang, W. Wang, H. Liang and H. Xu, *Cryst. Growth Des.*, 2009, **9**, 858–862.
66 Y. Yu, Q. Zhang, X. Lu and J. Y. Lee, *J. Phys. Chem. C*, 2010, **114**, 11119–11126.
67 A. Sanchez-Iglesias, I. Pastoriza-Santos, J. Perez-Juste, B. Rodriguez-Gonzalez, F. Abajo and L. M. Liz-Marzan, *Adv. Mater.*, 2006, **18**, 2529–2534.
68 J. Fuentes-García, J. Santoyo-Salzar, E. Rangel-Cortes, G. Goya, V. Cardozo-Mata and J. Pescador-Rojas, *Ultrason. Sonochem.*, 2020, **70**, 105274.
69 T. K. Sau and C. J. Murphy, *Langmuir*, 2004, **20**, 6414–6420.
70 H. A. Keul, M. Moeller and M. R. Bockstaller, *J. Phys. Chem. C*, 2008, **112**, 13483–13487.
71 S. Chen, Z. L. Wang, J. Ballato, S. H. Foulger and D. L. Carroll, *J. Am. Chem. Soc.*, 2004, **125**, 16186–16187.
72 H. L. Wu, C. H. Chen and M. H. Huang, *Chem. Mater.*, 2009, **21**, 110–114.
73 T. Wen, Z. Hu, W. Liu, H. Zhang, S. Hou, X. Hu and X. Wu, *Langmuir*, 2012, **28**, 17517–17523.
74 X. Xia, M. Yang, Y. Wang, Y. Zheng, Q. Li, J. Chen and Y. Xia, *ACS Nano*, 2012, **6**, 512–522.
75 Y. Wang, K. Sentosun, A. Li, M. Coronado-Puchau, A. Sánchez-Iglesias, S. Li, X. Su, S. Bals and L. M. Liz-Marzán, *Chem. Mater.*, 2015, **27**, 8032–8040.
76 J. Polte, T. T. Ahner, F. Delissen, S. Sokolov, F. Emmerling, A. F. Thunemann and R. Kraehnert, *J. Am. Chem. Soc.*, 2010, **132**, 1296–1301.
77 R. Shenhar, T. B. Norsten and V. M. Rotello, *Adv. Mater.*, 2005, **17**, 657–669.
78 F. Kim, J. H. Song and P. Yang, *J. Am. Chem. Soc.*, 2002, **124**, 14316–14317.
79 K. Okitsu, A. Yue, S. Tanabe, H. Matsumoto and Y. Yobiko, *Langmuir*, 2001, **17**, 7717–7720.
80 J. P. Sylvestre, S. Poulin, A. V. Kabashin, E. Sacher, M. Meunier and J. Luong, *J. Phys. Chem. B*, 2004, **108**, 16864–16869.
81 P. Prema, P. A. Iniya and G. Immanuel, *RSC Adv.*, 2016, **6**, 4601–4607.
82 M. Sengani, A. M. Grumezescu and V. D. Rajeswari, *OpenNano*, 2017, **2**, 37–46.
83 S. Mandal, S. Phadtare and M. Sastry, *Curr. Appl. Phys.*, 2005, **5**, 118–127.
84 X. Huang, S. Li, Y. Huang, S. Wu, X. Zhou, S. Li, C. L. Gan, F. Boey, C. Mirkin and H. Zhang, *Nat. Commun.*, 2011, **2**, 292.
85 Y. Cheng, J. Tao, G. Zhu, J. A. Soltis, B. A. Legg, N. Elias, Y. De, M. L. Sushko and J. Liu, *Nanoscale*, 2018, **10**, 11907–11912.
86 Y. Shimasaki, M. Kitahara, M. Shoji, A. Shimojima, H. Wada and K. Kuroda, *Chem.–Asian J.*, 2018, **13**, 3935–3941.
87 C. J. Murphy, A. M. Gole, S. E. Hunyadi and C. J. Orendorff, *Inorg. Chem.*, 2006, **45**, 7544–7554.
88 J. Tang, Q. Ou, H. Zhou, L. Qi and S. Man, *Nanomaterials*, 2019, **9**, 185.
89 Y. Xiong and Y. Xia, *Adv. Mater.*, 2007, **19**, 3385–3391.
90 S. G. Kwon, G. Krylova, P. J. Phillips, R. F. Klie, S. Chattopadhyay, T. Shibata, E. E. Bunel, Y. Liu, V. B. Prakapenka and B. Lee, *Nat. Mater.*, 2015, **14**, 215–223.
91 S. E. Habas, H. Lee, V. Radmilovic, G. A. Somorjai and P. Yang, *Nat. Mater.*, 2007, **6**, 692–697.
92 M. Grzelczak, J. Pérez-Juste, P. Mulvaney and L. Liz-Marzán, *Chem. Soc. Rev.*, 2008, **37**, 1783–1791.
93 W. Leng, P. Pati and P. J. Vikesland, *Environ. Sci.: Nano*, 2015, **2**, 440–453.
94 Z. Wei and C. J. Liu, *Mater. Lett.*, 2011, **65**, 353–355.
95 A. Dzimitrowicz, J. Piotr, G. Krzysztof, N. Piotr and P. Pohl, *J. Nanopart. Res.*, 2015, **17**, 185.
96 N. Saito, J. Hieda and O. Takai, *Thin Solid Films*, 2009, **518**, 912–917.
97 K. M. Koczkur, S. Mourdikoudis, L. Polavarapu and S. E. Skrabalak, *Dalton Trans.*, 2015, **44**, 17883–17905.
98 S. E. Skrabalak, L. Au, X. Li and Y. Xia, *Nat. Protoc.*, 2007, **2**, 2182–2190.
99 H. Wang, Z. Shan, K. D. Gilroy, Z. Cai and Y. Xia, *Nano Today*, 2017, **15**, 121–144.
100 R. S. Das, B. Singh, S. Mukhopadhyay and R. Banerjee, *Dalton Trans.*, 2012, **41**, 4641–4648.
101 J. Olesiak-Banska, M. Gordel, R. Kolkowski, K. Matczyszyn and M. Samoc, *J. Phys. Chem. C*, 2012, **116**, 13731–13737.
102 N. Wangoo, K. K. Bhasin, R. Boro and C. R. Suri, *Anal. Chim. Acta*, 2008, **610**, 142–148.
103 S. Yong, Y. Jin and S. Dong, *Chem. Commun.*, 2004, **10**, 1104–1105.
104 U. M. Badeggi, E. Ismail, A. O. Adeloye, S. Botha, J. A. Badmus, J. L. Marnewick, C. N. Cupido and A. A. Hussein, *Biomolecules*, 2020, **10**, 452.
105 A. Ahmeda, A. Zangeneh and M. M. Zangeneh, *Appl. Organomet. Chem.*, 2020, **34**, e5290.
106 P. Boomi, G. P. Poorani, S. Selvam, S. Palanisamy, S. Jegatheeswaran, K. Anand, C. Balakumar, K. Premkumar and H. G. Prabu, *Appl. Organomet. Chem.*, 2020, **34**, e5574.
107 S. Ahmad Khan, S. Shahid and C. S. Lee, *Biomolecules*, 2020, **10**, 835.

108 P. Ghosh, G. Han, M. De, C. K. Kim and V. M. Rotello, *Adv. Drug Delivery Rev.*, 2008, **60**, 1307–1315.
109 D. Cabuzu, A. Cirja, R. Puiu and A. Mihai Grumezescu, *Curr. Top. Med. Chem.*, 2015, **15**, 1605–1613.
110 T. Riddin, M. Gericke and C. Whiteley, *Nanotechnology*, 2006, **17**, 3482.
111 A. L. Ginzburg, L. Truong, R. L. Tanguay and J. E. Hutchison, *ACS Nano*, 2018, **12**, 5312–5322.
112 A. Sasidharan and N. Monteiro-Riviere, *Wiley Interdiscip. Rev.: Nanomed. Nanobiotechnol.*, 2015, **7**, 779–796.
113 M. J. Firdhouse and P. Lalitha, *Inorg. Chem. Commun.*, 2022, **143**, 109800.
114 P. Quaresma, L. Soares, L. Contar, A. Miranda, I. Osório, P. A. Carvalho, R. Franco and E. Pereira, *Green Chem.*, 2009, **11**, 1889–1893.
115 I. Bibi, N. Nazar, M. Iqbal, S. Kamal, H. Nawaz, S. Nourene, Y. Safa, K. Jilani, M. Sultan, S. Ata, F. Rehman and M. Abbas, *Adv. Powder Technol.*, 2017, **28**, 2035–2043.
116 N. Abdel-Raouf, N. M. Al-Enazi and I. B. M. Ibraheem, *Arabian J. Chem.*, 2017, **10**, S3029–S3039.
117 B. Khodadadi, M. Bordbar, A. Yeganeh-Faal and M. Nasrollahzadeh, *J. Alloys Compd.*, 2017, **719**, 82–88.
118 H. Veisi, M. Farokhia, M. Hamelian and S. Hemmati, *RSC Adv.*, 2018, **8**, 38186–38195.
119 P. Zhao, A. El-kott, A. E. Ahmed, A. Khames and M. A. Zein, *Inorg. Chem. Commun.*, 2021, **131**, 108781.
120 T. Ahmad, M. A. Bustam, M. Irfan, M. Moniruzzaman, H. M. A. Asghar and S. Bhattacharjee, *Mater. Chem. Phys.*, 2018, **220**, 240–248.
121 C. Tamuly, M. Hazarika, S. C. Borah, M. R. Das and M. P. Boruah, *Colloids Surf., B*, 2013, **102**, 627–634.
122 V. Kumar and S. K. Yadav, *J. Chem. Technol. Biotechnol.*, 2009, **84**, 151–157.
123 K. Cheirmadurai, S. Biswas, R. Muralia and P. Thanikaivelan, *RSC Adv.*, 2014, **4**, 19507–19511.
124 B. Khodadadi, M. Bordbar and M. Nasrollahzadeh, *J. Colloid Interface Sci.*, 2017, **490**, 1–10.
125 S. Ali, M. Iqbal, A. Naseer, M. Yaseen, I. Bibi, A. Nazir, M. I. Khan, N. Tamam, N. Alwadai, M. Rizwan and M. Abbasf, *Environ. Nanotechnol., Monit. Manage.*, 2021, **16**, 100511.
126 K. B. Narayanan and N. Sakthivel, *Adv. Colloid Interface Sci.*, 2010, **156**, 1–13.
127 M. Teimouri, F. Khosravi-Nejad, F. Attar, A. A. Saboury, I. Kostova, G. Benelli and M. Falahati, *J. Cleaner Prod.*, 2018, **184**, 740–753.
128 L. Gou and C. J. Murphy, *Chem. Mater.*, 2015, **17**, 3668–3672.
129 C. D. Dios, Y. F. Hua, F. García, A. Cebollada and G. Armelles, *Plasmonics*, 2018, **13**, 1–6.
130 Y. Y. Yu, S. S. Chang, C. L. Lee and C. Wang, *J. Phys. Chem. B*, 1997, **101**, 6661–6664.
131 A. Gole and C. J. Murphy, *Chem. Mater.*, 2004, **16**, 3633–3640.
132 N. R. Jana, *Chem. Commun.*, 2003, **15**, 1950–1951.
133 C. J. Orendorff and C. J. Murphy, *J. Phys. Chem. B*, 2006, **110**, 3990–3994.
134 M. Ali, B. Snyder and M. A. El-Sayed, *Langmuir*, 2012, **28**, 9807–9815.
135 S. Si, C. Leduc, M. H. Delville and B. Lounis, *ChemPhysChem*, 2012, **13**, 193–202.
136 J. Gao, C. M. Bender and C. J. Murphy, *Langmuir*, 2003, **19**, 9065–9070.
137 B. Nikoobakht and M. A. El-Sayed, *Langmuir*, 2001, **17**, 6368–6374.
138 S. Y. Lee, S. H. Jin, S. M. Kim and J. W. Kim, *Met. Mater. Int.*, 2014, **20**, 695–699.
139 N. R. Jana, L. Gearheart and C. J. Murphy, *Adv. Mater.*, 2001, **13**, 1389–1393.
140 A. P. Alivisatos, *J. Phys. Chem.*, 1996, **100**, 13226–13239.
141 M. Liu, A. Kira and H. Nakahara, *Langmuir*, 2003, **13**, 4807–4809.
142 T. H. Ha, H. J. Koo and B. H. Chung, *J. Phys. Chem. C*, 2007, **111**, 1123–1130.
143 C. J. Murphy, T. K. Sau, A. M. Gole, C. J. Orendorff, G. Jinxin, G. Linfeng, S. E. Hunyadi and L. Tan, *J. Phys. Chem. B*, 2005, **109**, 13857–13870.
144 B. D. Busbee, S. O. Obare and C. J. Murphy, *Adv. Mater.*, 2003, **15**, 414–416.
145 C. Wang, T. Wang, Z. Ma and Z. Su, *Nanotechnology*, 2005, **16**, 2555.
146 F. Kim, K. Sohn, J. Wu and J. Huang, *J. Am. Chem. Soc.*, 2008, **130**, 14442.
147 M. Grzelczak, A. Sanchez-Iglesias, B. Rodriguez-Gonzalez, R. Alvarez-Puebla, J. Perez-Juste and L. M. Liz-Marzan, *Adv. Funct. Mater.*, 2008, **18**, 3780–3786.
148 J. E. Millstone, W. Wei, M. R. Jones, H. Yoo and C. A. Mirkin, *Nano Lett.*, 2008, **8**, 2526–2529.
149 Z. R. Guo, C. R. Gu, X. Fan, Z. P. Bian, H. F. Wu, D. Yang, N. Gu and J. N. Zhang, *Nanoscale Res. Lett.*, 2009, **4**, 1428–1433.
150 J. Zhu, K. T. Yong, I. Roy, R. Hu, H. Ding, L. Zhao, M. T. Swihart, G. S. He, Y. Cui and P. N. Prasad, *Nanotechnology*, 2010, **21**, 285106.
151 L. Liu, Z. Guo, L. Xu, R. Xu and L. Xiang, *Nanoscale Res. Lett.*, 2011, **6**, 143.
152 X. Kou, S. Zhang, C. K. Tsung, Z. Yang, M. H. Yeung, G. Stucky, L. Sun, J. Wang and C. Yan, *Chem.–Eur. J.*, 2010, **13**, 2929–2936.
153 W. Ahmed, A. S. Bhatti and J. V. Ruitenbeek, *J. Nanopart. Res.*, 2017, **19**, 115.
154 S. Wang, N. Kristian, S. Jiang and W. Xin, *Electrochem. Commun.*, 2008, **10**, 961–964.
155 J. E. Millstone, S. Park, K. L. Shuford, L. Qin, G. C. Schatz and C. A. Mirkin, *J. Am. Chem. Soc.*, 2005, **127**, 5312–5313.
156 L. B. Rogers, D. P. Krause, J. C. Griess and D. B. Ehrlinger, *J. Electrochem. Soc.*, 1949, **95**, 33.
157 Z. Yang, Z. Li, X. Lu, F. He, X. Zhu, Y. Ma, R. He, F. Gao, W. Ni and Y. Yi, *Nano-Micro Lett.*, 2017, **9**, 5.
158 M. Z. Liu and P. Guyot-Sionnest, *J. Phys. Chem. B*, 2004, **108**, 5882–5888.
159 Z. Zhang, H. Li, F. Zhang, Y. Wu, Z. Guo, L. Zhou and J. Li, *Langmuir*, 2014, **30**, 2648–2659.

160 G. Weng, X. Dong, J. Li and J. Zhao, *J. Mater. Sci.*, 2016, **51**, 7678–7690.
161 Z. Chen, T. Balankura, K. A. Fichthorn and R. M. Rioux, *ACS Nano*, 2019, **13**, 1849–1860.
162 J. H. Lee, K. J. Gibson, C. Gang and Y. Weizmann, *Nat. Commun.*, 2015, **6**, 7571.
163 M. J. Schnepf, M. Mayer, C. Kuttner, M. Tebbe, D. Wolf, M. Dulle, T. Altantzis, P. Formanek, S. Förster and S. Bals, *Nanoscale*, 2017, **9**, 9376–9385.
164 A. H. Poghosyan, A. A. Shahinyan and J. Koetz, *Colloid Polym. Sci.*, 2018, **296**, 1301–1306.
165 A. H. Poghosyan, A. A. Shahinyan and J. Koetz, *Colloid Polym. Sci.*, 2018, **296**, 1301–1306.
166 C. Song, F. Li, W. Chen, X. Guo, D. Chen, J. Zhang, J. Zhang and L. H. Wang, *J. Mater. Chem. B*, 2019, **7**, 2001–2008.
167 P. Li, Y. Wu, D. Li, X. Su, C. Luo, Y. Wang, J. Hu, G. Li, H. Jiang and W. Zhang, *Nanoscale Res. Lett.*, 2018, **13**, 313.
168 S. Bandyopadhyay, B. H. McDonagh, G. Singh, K. Raghunathan, A. Sandvig, I. Sandvig, J. Andreassen and W. R. Glomm, *Nanoscale Res. Lett.*, 2018, **13**, 254.
169 G. Q. Tao and J. Wang, *Carbon*, 2018, **133**, 209–217.
170 R. Zhang, X. Zhang, L. I. Xiaoyu and P. Yang, *Funct. Mater. Lett.*, 2013, **6**, 1330003.
171 P. Yang, J. Wang and L. Zhang, *J. Cluster Sci.*, 2013, **24**, 399–426.
172 V. Biju, T. Itoh, A. Anas, A. Sujith and M. Ishikawa, *Anal. Bioanal. Chem.*, 2008, **391**, 2469–2495.
173 Y. Xianyu, Y. Xie, N. Wang, Z. Wang and X. Jiang, *Small*, 2015, **11**, 5510–5514.
174 P. M. Tiwari, K. Vig, V. A. Dennis and S. R. Singh, *Nanomaterials*, 2011, **1**, 31–63.
175 K. Niikura, T. Matsunaga, T. Suzuki, S. Kobayashi, H. Yamaguchi, Y. Orba, A. Kawaguchi, H. Hasegawa, K. Kajino, T. Ninomiya, K. Ijiro and H. Sawa, *ACS Nano*, 2013, **7**, 3926–3938.
176 N. L. Rosi and C. A. Mirkin, *Chem. Rev.*, 2010, **36**, 1547–1562.
177 C. L. Haynes and R. V. Duyne, *J. Phys. Chem. B*, 2001, **105**, 5599–5611.
178 S. L. Diedenhofen, D. Kufer, T. Lasanta and G. Konstantatos, *Light: Sci. Appl.*, 2015, **4**, 234.
179 Q. Zhang, Y. N. Tan, J. Xie and J. Y. Lee, *Plasmonics*, 2009, **4**, 9–22.
180 R. Elghanian, J. J. Storhoff, R. C. Mucic, R. L. Letsinger and C. Mirkin, *Science*, 1997, **277**, 1078–1081.
181 W. Sun, G. Wang, N. Fang and E. S. Yeung, *Anal. Chem.*, 2009, **81**, 9203.
182 E. Boisselier and D. Astruc, *Chem. Soc. Rev.*, 2009, **38**, 1759–1782.
183 A. Wang, C. J. Wu and S. H. Chen, *J. Proteome Res.*, 2006, **5**, 1488–1492.
184 W. P. Faulk and G. M. Taylor, *Immunochemistry*, 1971, **8**, 1081–1083.
185 J. H. W. Leuvering, P. J. H. M. Thal, M. v. d. Waart and A. H. W. M. Schuurs, *Fresenius' Zeitschrift für analytische Chemie*, 1980, **301**, 132.
186 C. A. Mirkin, R. L. Letsinger, R. C. Mucic and J. J. Storhoff, *Nature*, 1996, **382**, 607–609.
187 L. Di, Y. Yan, A. Wieckowska and I. Willner, *Chem. Commun.*, 2007, **34**, 3544–3546.
188 X. M. Li, P. Y. Fu, J. M. Liu and S. S. Zhang, *Anal. Chim. Acta*, 2010, **673**, 133–138.
189 N. G. Khlebtsov, *Quantum Electron.*, 2008, **38**, 504–529.
190 W. R. Glomm, *J. Dispersion Sci. Technol.*, 2005, **26**, 389–414.
191 Z. Krpetic, P. Nativo, F. Porta and M. Brust, *Bioconjugate Chem.*, 2009, **20**, 619–624.
192 L. A. Dykman and V. A. Bogatyrev, *Russ. Chem. Rev.*, 2010, **76**, 181.
193 P. Maity, S. Xie, M. Yamauchi and T. Tsukuda, *Nanoscale*, 2012, **4**, 4027–4037.
194 D. Zhu, D. Xing, X. Shen and G. Yan, *Chin. Sci. Bull.*, 2003, **48**, 1741–1744.
195 W. He, C. Z. Huang, Y. F. Li, J. P. Xie, R. G. Yang, P. F. Zhou and J. Wang, *Anal. Chem.*, 2008, **80**, 8424–8430.
196 H. Li and L. Rothberg, *Proc. Natl. Acad. Sci. U. S. A.*, 2004, **101**, 14036–14039.
197 Q. Dai, L. Xiong, J. Coutts, L. Austin and Q. Huo, *J. Am. Chem. Soc.*, 2008, **130**, 8138–8139.
198 D. A. Gell, R. P. Grant and J. P. Mackay, *Adv. Exp. Med. Biol.*, 2012, **747**, 19–41.
199 H. Li and L. Rothberg, *Anal. Chem.*, 2005, **77**, 6229–6233.
200 J. D. Watson and S. Devons, *Phys. Today*, 1968, **21**, 71–72.
201 E. Papadopoulou, N. Gale, J. F. Thompson, T. A. Fleming, T. Brownc and P. N. Bartlett, *Chem. Sci.*, 2016, **7**, 386–393.
202 X. Lin, A. P. Ivanov and J. B. Edel, *Chem. Sci.*, 2017, **8**, 3905–3912.
203 T. A. Taton, C. A. Mirkin and R. L. Letsinger, *Science*, 2000, **289**, 1757–1760.
204 H. R. Sim, A. W. Wark and H. J. Lee, *Analyst*, 2010, **135**, 2528–2532.
205 C. Nietzold and F. Lisdat, *Analyst*, 2012, **137**, 2821–2826.
206 E. Yasun, B. Gulbakan, I. Ocsoy, Y. Quan and W. Tan, *Anal. Chem.*, 2012, **84**, 6008–6015.
207 Y. Wang, D. Li, W. Ren, Z. Liu and S. Dong, *Chem. Commun.*, 2008, **22**, 2520–2522.
208 H. Jans, X. Liu, L. Austin, G. Maes and Q. Huo, *Anal. Chem.*, 2009, **81**, 9425–9432.
209 S. Link, M. B. Mohamed and M. A. El-Sayed, *J. Phys. Chem. B*, 1999, **103**, 3073–3077.
210 M. Rex, F. E. Hernandez and A. D. Campiglia, *Anal. Chem.*, 2006, **78**, 445–451.
211 H. Nakashima, K. Furukawa, Y. Kashimura and K. Torimitsu, *Chem. Commun.*, 2007, **10**, 1080–1082.
212 P. K. Sudeep, S. Joseph and K. G. Thomas, *J. Am. Chem. Soc.*, 2005, **127**, 6516–6517.
213 M. Li, J. Woongkang, S. Sukumar, R. Raodasari and I. Barman, *Chem. Sci.*, 2015, **6**, 3906–3914.
214 X. Huang, I. H. El-Sayed, Q. Wei and M. A. El-Sayed, *J. Am. Chem. Soc.*, 2006, **128**, 2115–2120.
215 E. Dujardin, S. Mann, L. B. Hsin and C. Wang, *Chem. Commun.*, 2001, **14**, 1264–1265.
216 I. C. Pekcevik, L. Poon, M. Wang and B. D. Gates, *Anal. Chem.*, 2013, **85**, 9960–9967.

217 S. J. Zhen, F. L. Guo, L. I. Yuanfang and C. Z. Huang, *Sci. China: Chem.*, 2013, **56**, 387–392.
218 H. Li and L. Rothberg, *J. Am. Chem. Soc.*, 2004, **126**, 10958–10961.
219 H. C. Huang, S. Barua, D. B. Kay and K. Rege, *ACS Nano*, 2010, **4**, 1769–1770.
220 A. Wijaya, S. B. Schaffer, I. G. Pallares and K. Hamad-Schifferli, *ACS Nano*, 2009, **3**, 80–86.
221 V. Baumann, P. Röttgermann, F. Haase, K. Szendrei, P. Dey, K. Lyons, R. Wyrwich, M. Gräßel, J. Stehr, L. Ullerich, F. Bürsgensd and J. Rodríguez-Fernández, *RSC Adv.*, 2016, **6**, 103724–103739.
222 W. Ma, H. Kuang, L. Xu, L. Ding, C. Xu, L. Wang and N. A. Kotov, *Nat. Commun.*, 2013, **4**, 2689.
223 D. Ho, J. A. Kretzmann, M. Norret, P. Toshniwal, J. P. Veder, H. Jiang, P. Guagliardo, A. M. Munshi, R. Chawla and C. W. Evans, *Nat. Nanotechnol.*, 2018, **13**, 1148–1153.
224 K. J. Lee, H. M. So, B. K. Kim, D. W. Kim and J. H. Jang, *J. Nanomater.*, 2011, **2**, 1–8.
225 Y. Bao, L. Vigderman, E. R. Zubarev and C. Jiang, *Langmuir*, 2012, **28**, 923–930.
226 S. W. Liu, L. Wang, M. Lin, Y. Liu, L. N. Zhang and H. Zhang, *Chin. J. Polym. Sci.*, 2019, **37**, 115–128.
227 S. Wang, H. Xu and J. Ye, *Phys. Chem. Chem. Phys.*, 2014, **16**, 12275–12281.
228 D. P. O'Neal, L. R. Hirsch, N. J. Halas, J. D. Payne and J. L. Westb, *Cancer Lett.*, 2004, **209**, 171–176.
229 X. Huang, I. H. El-Sayed, Q. Wei and M. A. El-Sayed, *J. Am. Chem. Soc.*, 2006, **128**, 2115–2120.
230 Y. Wang, X. Ji, P. Pang, Y. Shi, J. Dai, J. Xu, J. Wu, T. B. Kirk and W. Xue, *J. Mater. Chem. B*, 2018, **6**, 2481–2488.
231 W. Xu, J. Qian, G. Hou, Y. Wang, J. Wang, T. Sun, L. Ji, A. Suo and Y. Yao, *Acta Biomater.*, 2049, **83**, 400–413.
232 T. Yang, D. Wang and X. Liu, *Colloids Surf., B*, 2019, **173**, 833–841.